Carbohydrate Polymers 238 (2020) 116183

Contents lists available at ScienceDirect

Carbohydrate Polymers

journal homepage: www.elsevier.com/locate/carbpol

Effects of simulated saliva-gastrointestinal digestion on the physicochemical properties and bioactivities of okra polysaccharides

Qin Yuan[a,1], Yuan He[a,1], Pan-Yin Xiang[a], Sheng-Peng Wang[b], Zheng-Wen Cao[a], Tao Gou[a], Miao-Miao Shen[a], Li Zhao[a], Wen Qin[a], Ren-You Gan[c,*], Ding-Tao Wu[a,*]

[a] Institute of Food Processing and Safety, College of Food Science, Sichuan Agricultural University, Ya'an 625014, Sichuan, China
[b] State Key Laboratory of Quality Research in Chinese Medicine, Institute of Chinese Medical Sciences, University of Macau, Macao
[c] Institute of Urban Agriculture, Chinese Academy of Agricultural Sciences, Chengdu 610213, China

ARTICLE INFO

Keywords:
Okra polysaccharides
In vitro digestion
Physicochemical properties
Antioxidant activity
Enzyme inhibition
Prebiotic activity

ABSTRACT

This study was to investigate the effects of *in vitro* simulated saliva-gastrointestinal digestion on the physicochemical properties and bioactivities of okra polysaccharides (OPS). Results showed that the digestibilities of OPS were about 5.1%, 37.5%, and 41.3% after saliva digestion (SD), saliva-gastric digestion (SGD), and saliva-gastrointestinal digestion (SGID), respectively. The SGID significantly changed the physicochemical properties of OPS, such as total uronic acids, total flavonoids, monosaccharide composition, rheological properties, and molecular weights (M_w). Especially, M_w changes resulted in the breakdown of glycosidic bonds during SGD, and the degradation of OPS during SGID was mainly caused by disrupting aggregates. Furthermore, the bioactivities of OPS were also affected by SGID. After SGID, OPS still possessed strong antioxidant activities, binding capacities, and prebiotic activities, but the α-glucosidase inhibitory effect was obviously decreased. Overall, results can provide valuable and scientific support on the oral administration of OPS as functional foods and medicines in the future.

1. Introduction

Okra (*Abelmoschus esculentus* (L.) Moench), an annual plant originating from the African region, has been cultivated all around the world in recent decades, mainly in tropical and subtropical areas (Liu, Wang, Yong, Kan, & Jin, 2018; Liu, Zhao et al., 2018; Shen et al., 2019). Recently, okra is also widely planted in China (Nie et al., 2019). It is not only consumed as a seasonal vegetable, but also used as folk medicine in China (Gao et al., 2018). Due to a variety of health benefits, okra has attracted increasing research interests. Especially, previous studies have demonstrated that polysaccharides abundantly exist in the okra fruit, ranging from about 10.4% to 16.9% (Yuan, Lin et al., 2019; Yuan, Li et al., 2019). Moreover, okra polysaccharides have been reported to possess relatively high molecular weights ranging from 2.76×10^6 to 6.59×10^6 Da (Nie et al., 2019; Yuan, Lin et al., 2019; Yuan, Li et al., 2019). The relatively high content of uronic acids in okra polysaccharides confirms the presence of pectic-polysaccharides. The major monosaccharide composition of pectic-polysaccharides in okra includes galactose, rhamnose, arabinose, and galacturonic acid (Liu, Wang et al., 2018; Liu, Zhao et al., 2018; Olawuyi, Kim, Hahn, & Lee, 2020). Furthermore, rhamnogalacturonan-I (RG-I) segments with varying branching chain composition have been identified as the major pectic-polysaccharides in okra fruit. Actually, pectic-polysaccharides are considered as the main active ingredients in okra fruit, possessing multiple bioactivities, such as antioxidant (Yuan et al., 2020), anti-obesity (Nie et al., 2019), and hypoglycemic effects (Liu, Wang et al., 2018; Liu, Zhao et al., 2018). Hence, okra polysaccharides have potential applications in functional foods, health care, and pharmaceutical industries.

The *in vitro* digestion model is a convenient, economical, and reproducible tool to study the digestibility, chemical and structural changes, and release of food components in the human intestines (Hu, Nie, Min, & Xie, 2013; Hur, Lim, Decker, & McClements, 2011). This model can simulate the transport of food components in the human digestive tract by sequentially exposing substances to simulated oral, stomach, and small intestinal conditions (Hu et al., 2013). In this model, mobilization of the substances is simulated under the same conditions of salt solution, pH, and digestive enzymes in the saliva, gastric, and intestine. Previous studies have shown that the pH, bile salts, and digestive enzymes in the mimic digestive juice may change

* Corresponding authors.
E-mail addresses: ganrenyou@caas.cn (R.-Y. Gan), DT_Wu@sicau.edu.cn (D.-T. Wu).
[1] These authors contributed equally to this work.

https://doi.org/10.1016/j.carbpol.2020.116183
Received 18 December 2019; Received in revised form 12 March 2020; Accepted 14 March 2020
Available online 25 March 2020
0144-8617/

the physicochemical properties, such as molecular weight, viscosity, chemical composition, surface morphology, and conformation, and biological activities, such as antioxidant activity as well as α-amylase and α-glucosidase inhibitory activities of polysaccharides from natural resources (Chen et al., 2016; Hu et al., 2013; Li, Wang, Yuan, Pan, & Chen, 2018; Wang et al., 2018; Zhu et al., 2019). However, whether the physicochemical properties and bioactivities of okra polysaccharides can be influenced by the gastrointestinal digestion remains unknown, and the investigation of their potential digestion mechanism is necessary.

Therefore, it is important to study the effects of *in vitro*saliva-gastrointestinal digestion on the physicochemical properties and bioactivities of okra polysaccharides. This study was aimed to evaluate the influences of *in vitro* saliva-gastrointestinal digestion on the physicochemical properties, antioxidant activities, binding capacities, inhibitory activity on α-glucosidase, and prebiotic activities of okra polysaccharides.

2. Materials and methods

2.1. Materials and chemicals

Okra fruits (*A. esculentus* cv. Wufu) were collected in Chengdu, Sichuan Province, China. Pepsin (3000 U/g), pancreatin (4000 U/g), carboxymethyl cellulose, 2,2-azino-Bis (3-ethylbenzthiazoline-6-sulphonic acid) (ABTS), griess reagent, sodium nitroprusside (SNP), 2,2-diphenyl-1-(2,4,6-trinitrophenyl) hydrazyl (DPPH), acarbose, α-glucosidase (10 U/mg), and 4-nitrophenyl β-D-glucopyranoside were purchased from Sigma-Aldrich (St. Louis, MO, USA). A free cholesterol assay kit and Man-Rogosa-Sharpe (MRS) medium were purchased from Solarbio Science (Beijing, China). Furthermore, three *Lactobacillus* strains, including *L. rhamnosus* CICC 6133, *L. rhamnosus* CICC 6151, and *L. acidophilus* CICC 6089, were purchased from China Center of Industrial Culture Collection. All other chemicals and reagents used were of analytical grade.

2.2. Preparation of polysaccharides from okra fruits

Hot-water extraction of okra polysaccharides (OPS) was performed based on the formerly reported method (Yuan, Lin et al., 2019; Yuan, Li et al., 2019). Briefly, the OPS was extracted twice with a phosphate buffer (50 mM, pH 6.0) solution (1: 30, *w/v*) at 95 °C for 1 h. Then, the crude okra polysaccharides were alcohol precipitated, dialyzed, lyophilized, and stored at -20 °C for further analysis.

2.3. In vitro simulated saliva-gastrointestinal digestion of OPS

The *in vitro* simulated saliva-gastrointestinal digestion of OPS was performed based on the former methods with slight modifications (Wang et al., 2018). Briefly, 10.0 mL of OPS solution (6.0 mg/mL) was mixed with 10.0 mL of simulated saliva juice, and incubated in a steam bath oscillation at 37 °C. Samples (2.0 mL) were collected at 0.25 h, 0.5 h, and 1.0 h of incubation, and then boiled in a water bath for 10 min to inactivate enzymes. After the saliva digestion, the mixture of 10.0 mL of saliva digested samples and 10.0 mL of simulated gastric fluid was further incubated at 37 °C, and the pH of the mixture was maintained at 2.0. Next, saliva-gastric digested samples (2.0 mL) were again collected at 0.5, 1.0, 2.0, 4.0, and 6.0 h of incubation with following procedures performed as the saliva digestion. Furthermore, after the saliva-gastric digestion, the OPS solution was mixed with the artificial small intestinal juice at a ratio of 10: 3 (*v/v*), and incubated at 37 °C, and the pH of the mixture was adjusted to 6.8. After that, digested samples (2.0 mL) were collected at 0.5, 1.0, 2.0, 4.0, and 6.0 h of incubation with following procedures performed as the saliva digestion.

All digested samples were centrifuged, and the supernatants were used for the measurement of reducing sugar contents (Hu et al., 2013). And the supernatants were precipitated with four volumes of 95% (*v/v*) ethanol, dialyzed, and lyophilized to obtain the saliva digested samples (OPS-S), saliva-gastric digested samples (OPS-G), and saliva-gastrointestinal digested samples (OPS-I), respectively.

2.4. Determination of physicochemical properties of OPSs

2.4.1. Analysis of chemical components of OPSs

The total polysaccharides, uronic acids, proteins, phenolics, and flavonoids of OPSs were measured by our formerly reported methods (Nie et al., 2019; Yuan et al., 2020). Briefly, the total polysaccharides in OPSs (%, *w/w*) were determined by the phenol-sulfuric acid method with a mixed reference composed of 70% of galactose and 30% of galacturonic acid. The total uronic acids in OPSs (%, *w/w*) were determined by the *m*-hydroxydiphenyl method with galacturonic acid as a reference. The total proteins in OPSs (%, *w/w*) were determined by the Bradford's method with bovine serum albumin as a reference. Furthermore, the total phenolic content (TPC) in OPSs was determined by using gallic acid as a reference, which was expressed as mg of gallic acid equivalent per gram of OPSs. The total flavonoid content (TFC) in OPSs was determined by using ruin as a reference, which was expressed as mg of rutin equivalent per gram of OPSs.

2.4.2. Determination of molecular weights and monosaccharide compositions of OPSs

The molecular weights (M_w) and polydispersities (M_w/M_n) of OPSs were determined by high performance size exclusion chromatography coupled with multi angle laser light scattering and refractive index detector (HPSEC-MALLS-RID, Wyatt Technology Co., Santa Barbara, CA, USA) according to the former method (Wu et al., 2016). The Shodex OHpak SB-806 M HQ (300 mm × 8.0 mm, i.d.) column was used for the separation of OPSs at 30 °C. Furthermore, the high performance liquid chromatography (HPLC, U3000, ThermoFisher, Waltham, MA, USA) equipped with a Phenomenex gemini 5 u C18 110A (150 mm × 4.6 mm, 5 μm) column was also used for the analysis of monosaccharide compositions in OPSs by the formerly reported method (Yuan, Lin et al., 2019; Yuan, Li et al., 2019).

2.4.3. Fourier transform infrared spectroscopy analysis of OPSs

The fourier transform infrared (FT-IR) analysis of OPSs was performed by a Nicolet iS 10 FT-IR (ThermoFisher Scientific, Waltham, MA, USA) based on the formerly reported method (Wu et al., 2014).

2.4.4. Rheological characterization of OPSs

Rheological properties of OPSs (4.0 mg/mL) were determined at 25.0 ± 0.1 °C by using a Discovery Hybrid Rheometer-1 (DHR-1, TA Instruments, New Castle DE, USA) according to the formerly reported method (Yuan et al., 2020).

2.5. Evaluation of bioactivities of OPSs

2.5.1. In vitro antioxidant activities

The ABTS and nitric oxide (NO) radical scavenging activities, and the ferric reducing antioxidant powers (FRAP) of OPSs were determined by previously reported methods (Guo et al., 2019). BHT or vitamin C was used as the positive control. Each sample was detected at five different concentrations, and a logistic regression curve was established to calculate the IC_{50} value (mg/mL).

2.5.2. In vitro binding properties

The *in vitro* binding capacities of OPSs were also measured by previously reported methods (Fu et al., 2019). The fat, cholesterol, and bile acid binding capacities of OPSs were expressed as gram of binding fat per gram of OPSs (g/g), milligram of binding cholesterol per gram of OPSs (mg/g), and a percent of blank control (%), respectively.

2.5.3. In vitro α-glucosidase inhibitory effect

The α-glucosidase inhibitory activities of OPSs were carried out by the formerly reported method (Yuan, Lin et al., 2019; Yuan, Li et al., 2019). Each sample was measured at five different concentrations, and acarbose was used as the positive control. A logistic regression curve was used to calculate the IC_{50} value (μg/mL).

2.5.4. In vitro prebiotic activities

The prebiotic activities of OPSs were measured by the formerly reported method with minor modifications (Huang et al., 2019). Carbohydrate-free MRS broth was used to determine whether the OPSs could promote the growth of *Lactobacillus* strains, including *L. acidophilus* CICC 6089, *L. rhamnosus* CICC 6133, and *L. rhamnosus* CICC 6151. Inulin was used as the positive control. Each sample after filter-sterilization was added into the basal MRS at the final concentration of 1.0% (*w/v*). Then, each *Lactobacillus* strain was inoculated in the medium containing polysaccharides to reach the concentration of 1×10^7 CFU/mL, and incubated at 37 °C (*L. rhamnosus* CICC 6151 and *L. acidophilus* CICC 6089) or 30 °C (*L. rhamnosus* CICC 6133) for 24 h. Finally, the optical density values at 600 nm were determined. The total short-chain fatty acids (SCFAs) in the culture medium were measured by the method reported with slight modifications (Di et al., 2018). Agilent 7890B GC system (Agilent Technologies Inc., Santa Clara, CA, USA) equipped with a flame ionization detector and an HP-INNOWax column (30 m × 250 μm × 0.25 μm, Agilent Technologies Inc., Santa Clara, CA, USA) was performed for the determination of SCFAs.

2.6. Statistical analysis

All the experiments were performed in triplicates, and the results were expressed as mean ± standard deviation. Statistical analysis was performed by using Origin 9.0 software (OriginLab Corporation, Northampton, Mass., USA). Statistical significances were carried out by one-way analysis of variance (ANOVA) plus *post hoc* Duncan's test. Statistical significance was defined at $p < 0.05$.

3. Results and discussion

3.1. Effects of in vitro saliva-gastrointestinal digestion on the physicochemical properties of OPS

3.1.1. Changes of reducing sugar contents and chemical compositions of OPS during digestion

The breakdown of glycosidic bonds of polysaccharides can lead to the increase of the number of reducing ends, resulting in a decrease in their molecular weights (Chen et al., 2012). Fig. 1 shows the changes of reducing sugar contents (C_R) of OPS during the saliva-gastrointestinal digestion. As shown in Fig. 1, after gastrointestinal digestion, a significant increase of C_R was observed. The C_R of OPS had no significant difference during the saliva digestion, indicating that OPS could not be hydrolyzed by the saliva juice. In fact, most natural non-starch polysaccharides cannot be digested by human saliva (Chen et al., 2018). However, the C_R sharply increased to 0.47 ± 0.01 mg/mL after gastric digestion for 30 min, which might attribute to the breakdown of glycosidic bonds and the formation of reducing ends at pH 2.0 (Hu et al., 2013). Then, the C_R slightly decreased from gastric digestion to intestinal digestion due to a diluted effect by the intestinal juice, indicating that no obvious reducing ends were produced during the intestinal digestion. In addition, the changes found in C_R were also consistent with the digestibility of OPS (Table 1).

The effects of saliva-gastrointestinal digestion on the digestibility and contents of different chemical components of OPS are summarized in Table 1. The digestibilities of OPS digested by saliva digestion (SD), saliva-gastric digestion (SGD), and saliva-gastrointestinal digestion (SGID) were detected as 5.1%, 37.5%, and 41.3%, respectively, indicating that OPS was mainly degraded in the stomach, probably due to the extremely low pH of gastric fluid (Hu et al., 2013). The contents of total polysaccharides, uronic acids, and proteins in OPS were detected as 87.53% ± 4.16%, 32.86% ± 3.04%, and 3.47% ± 0.16%, respectively, consistent with the results of previous studies (Nie et al., 2019; Yuan, Lin et al., 2019; Yuan, Li et al., 2019; Yuan et al., 2020). After gastrointestinal digestion, the contents of total polysaccharides, uronic acids, and total flavonoids in OPS-I significantly ($p < 0.05$) decreased by 6.07%, 25.19%, and 36.76% compared with OPS, respectively. This result might be related to the low pH during the gastric digestion, consistent with previous results that the reduction of contents of total polysaccharides and uronic acids in polysaccharides after gastrointestinal digestion might be related to low pH and enzymes (Wang et al., 2018). Besides, the contents of total phenolics significantly reduced during the gastric digestion. This result might be due to the release of bound phenolic compounds under pepsin and low pH conditions, and then free phenolic compounds were dialyzed off (Quan et al., 2018). However, the contents of total phenolics slightly increased after the gastrointestinal digestion, which might be related to the re-conjugation of free phenolic compounds with polysaccharides in the alkaline solution, which could enhance the antioxidant activity of OPS (Hosseini, Khodaiyan, Kazemi, & Najari, 2019; Liu, Wang et al., 2018; Liu, Zhao et al., 2018).

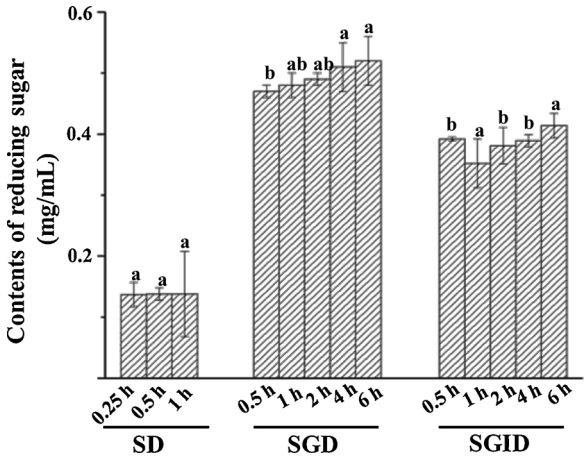

Fig. 1. Changes of reducing sugar contents of okra polysaccharides during digestion.
SD, saliva digestion; SGD, saliva-gastric digestion; SGID, saliva-gastrointestinal digestion; Means were compared in different groups, and different lowercase letters indicated statistical significance ($p < 0.05$).

3.1.2. Changes of molecular weights and monosaccharide compositions of OPS during digestion

The bioactivities of natural polysaccharides are related to their molecular weights and monosaccharide compositions (Wu et al., 2018). Therefore, the effects of saliva-gastrointestinal digestion on the molecular weights and monosaccharide compositions of OPS were next investigated. Fig. 2A showed the HPSEC-RID chromatograms of OPS, OPS-S, OPS-G, and OPS-I. There were four polysaccharide fractions (fractions 1 to 4) determined in OPS, OPS-S, OPS-G, and OPS-I, respectively. After SD, the molecular weight distribution of OPS did not change significantly. However, after gastrointestinal digestion, the molecular weight distribution of OPS changed significantly (Fig. 2A). The detailed molecular weights, relative peak areas (%), and molecular weight distributions of fractions 1-4 in OPS, OPS-S, OPS-G, and OPS-I are summarized in Table 2. After SD, the relative peak area of fraction 3 significantly decreased to 18.6%, resulting in a slight increase in the relative peak area of fraction 1 (Table 2). In addition, the fraction 3 of OPS changed slightly in the saliva juice, while the fractions 1, 2, and 4 of OPS remained stable. However, after SGD, the molecular distribution of OPS changed significantly as the addition of gastric fluid. The

Table 1
Changes of digestibility and contents of total polysaccharides, uronic acids, proteins, and phenolics of okra polysaccharides during digestion.

	OPS	OPS-S	OPS-G	OPS-I
Digestibility (%, *w/w*)	-	5.1%	37.5%	41.3%
Total polysaccharides (%, *w/w*)	87.53 ± 4.16 [a]	90.18 ± 3.09 [a]	79.07 ± 4.56 [b]	82.21 ± 4.86 [b]
Total uronic acids (%, *w/w*)	32.86 ± 3.04 [b]	36.12 ± 3.13 [a]	26.17 ± 3.42 [c]	24.58 ± 2.39 [c]
Degree of esterification (%)	23.86 ± 2.16 [b]	22.09 ± 2.72 [b]	37.99 ± 1.40 [a]	24.73 ± 0.94 [b]
Total proteins (%, *w/w*)	3.47 ± 0.16 [b]	3.67 ± 0.13 [b]	2.09 ± 0.14 [c]	5.90 ± 0.32 [a]
TPC (mg GAE/g)	12.84 ± 0.72 [b]	10.02 ± 0.26 [c]	10.79 ± 0.32 [c]	15.13 ± 0.79 [a]
TFC (mg RE/g)	9.88 ± 0.47 [a]	9.28 ± 0.52 [a]	4.86 ± 0.35 [b]	4.15 ± 0.50 [b]

Digestibility (%, *w/w*), the content of OPS digested during digestion; Total polysaccharides (%, *w/w*), total uronic acids (%, *w/w*), and total proteins (%, *w/w*), the total content of neutral and acidic polysaccharides, the total content of uronic acids, and the total content of proteins in OPSs, respectively; Degree of esterification (%), the esterification degree of total uronic acids; TPC, total phenolic content, mg of gallic acid equivalent per gram of OPSs; TFC, total flavonoid content, mg of rutin equivalent per gram of OPSs; Values represent mean ± standard deviation, and different superscript lowercase letters indicated significance ($p < 0.05$) in each row.

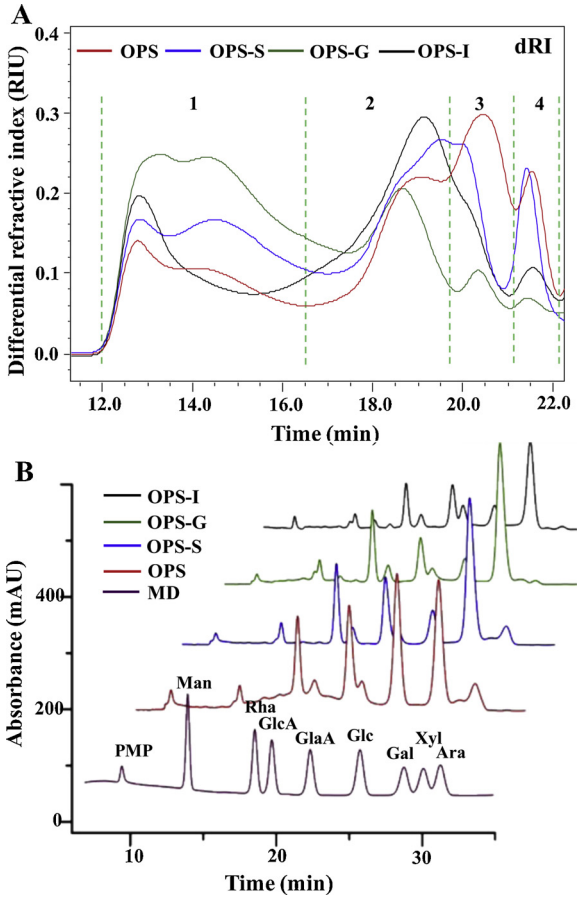

Fig. 2. Changes of high performance size exclusion chromatograms (A) and high performance liquid chromatography profiles of monosaccharide compositions (B) of okra polysaccharides during digestion.
OPS, okra polysaccharides; OPS-S, OPS-G, and OPS-I, OPS digested by saliva digestion, saliva-gastric digestion, and saliva-gastrointestinal digestion, respectively; In Fig. 2A, "1-4" indicated fractions 1-4 of OPS, OPS-S, OPS-G, and OPS-I; PMP, 1-phenyl-3-methyl-5-pyrazolone; Man, mannose; Rha, rhamnose; GlcA, glucuronic acid; GalA, galacturonic acid; Glc, glucose; Gal, galactose; Xyl, xylose; Ara, arabinose.

relative peak areas of fractions 2, 3, and 4 were reduced to 25.7%, 8.3% and 3.8%, respectively, resulting in an increase of the relative peak area of fraction 1 (62.2%), suggesting that the structures of fractions 2, and 3, and 4 of OPS were degraded by the gastric fluid. Furthermore, after SGID, the relative peak area of fraction 1 significantly reduced to 37.9%, resulting in an increase of relative peak areas of fractions 2 and 3, suggesting that OPS was further degraded in the intestinal digestion.

Table 2
Changes of molecular weight (M_w), polydispersity (M_w/M_n), and molar ratio of monosaccharide compositions of okra polysaccharides during digestion.

	OPS	OPS-S	OPS-G	OPS-I
M_w (Da)				
Fraction 1 × 10^6	3.33 (± 0.11) [b]	3.12 (± 0.09) [b]	2.55 (± 0.09) [c]	4.02 (± 0.18) [a]
Relative peak areas (%)	31.9	43.7	62.2	37.9
Fraction 2 × 10^5	2.10 (± 0.14) [a]	1.62 (± 0.05) [b]	2.25 (± 0.14) [a]	2.41 (± 0.11) [a]
Relative peak areas (%)	27.2	28.8	25.7	38.1
Fraction 3 × 10^4	3.62 (± 0.21) [c]	4.97 (± 0.18) [c]	15.97 (± 1.09) [a]	13.37 (± 0.36) [b]
Relative peak areas (%)	29.1	18.6	8.3	17.4
Fraction 4 × 10^4	2.86 (± 0.16) [b]	4.26 (± 0.17) [b]	15.70 (± 1.01) [a]	15.28 (± 0.33) [a]
Relative peak areas (%)	11.8	8.8	3.8	6.6
M_w/M_n				
Fraction 1	1.35	1.73	1.64	1.43
Fraction 2	1.53	1.43	1.18	1.39
Fraction 3	1.07	1.07	1.03	1.06
Fraction 4	1.07	1.19	1.01	1.01
Monosaccharide compositions and molar ratios				
Rhamnose	1.00	1.00	1.00	1.00
Galactose	1.83	2.59	2.07	2.23
Galacturonic acid	1.41	1.20	0.77	1.19
Glucose	1.13	0.70	0.44	0.85
Glucuronic acid	0.24	0.24	0.26	0.28
Mannose	0.12	0.10	0.20	0.18
Arabinose	0.46	0.34	-	-

Values represent mean ± standard deviation, and different superscript lowercase letters indicated statistical significance ($p < 0.05$) in each row. Fractions 1 to 4 were the same as in the Fig. 2A.

Compared with the SGD, the C_R remained stable during SGID (Fig. 1), indicating that the degradation of fraction 1 during SGID might be due to the disruption of aggregates, consistent with a previous study (Yuan, Lin et al., 2019; Yuan, Li et al., 2019). As shown in Table 2, the molecular weights of fractions 1, 2, 3, and 4 in OPS, OPS-S, OPS-G, and OPS-I ranged from 2.55 × 10^6 to 4.02 × 10^6 Da, from 1.62 × 10^5 to 2.41 × 10^5 Da, from 3.62 × 10^4 to 15.97 × 10^4 Da, and from 2.86 × 10^4 to 15.70 × 10^4 Da, respectively. This result was similar to the previous study that *in vitro* simulated digestion significantly affected the molecular weights of natural polysaccharides (Zhu et al., 2019). After SD, the molecular weights of OPS-S did not change significantly when compared with OPS, in agreement with the C_R of OPS-S during saliva digestion, which indicated that the saliva juice had no significant influence on the molecular weights of OPS. Similar results have been observed in previous studies that some polysaccharides were stable

during saliva digestion (Hu et al., 2013). However, after SGD, the molecular weight of fraction 1 in OPS-G significantly ($p < 0.05$) decreased, which was determined at 2.55 × 10^6 Da, in agreement with previous studies that natural polysaccharides could be degraded in the gastric juice (Carnachan, Bootten, Mishra, Monro, & Sims, 2012). Besides, the C_R of OPS-G sharply increased during gastric digestion, confirming that the reduction of molecular weights of OPS-G was due to the breakdown of glycosidic bonds (Chen et al., 2016). However, after SGID, the molecular weight of fraction 1 in OPS-I significantly ($p < 0.05$) increased, which was detected at 4.02 × 10^6 Da. The result might be attributed to the reduction of relatively low molecular weight fraction (fraction eluted from about 14.0 to 16.5 min) in fraction 1, resulting in a relative increase of high molecular weight fraction (fraction eluted from about 12.0 to 14.0 min) in fraction 1 (Fig. 2A). Besides, the presence of a number of salts in the gastrointestinal solution might cause the co-precipitation of polysaccharides together with other impurities, resulting in a relatively high molecular weight of fraction 1 in OPS-I (Hu & Goff, 2018). However, our result was different from a previous report that the molecular weights of tea polysaccharides could be further degraded by intestinal digestion (Li et al., 2018). Furthermore, the polydispersities of fractions 1, 2, 3, and 4 in OPS, OPS-S, OPS-G, and OPS-I ranged from 1.35 to 1.73, from 1.18 to 1.53, from 1.03 to 1.07, and from 1.01 to 1.19, respectively, consistent with the HPSEC chromatograms.

A monosaccharide is the natural basic unit, which influences the distinct structures and properties of polysaccharides. The analysis of monosaccharide compositions plays a crucial role in the structural characterization of polysaccharides. Fig. 2B showed the HPLC-UV profiles of monosaccharide compositions in OPS, OPS-S, OPS-G, and OPS-I. Results indicated that the HPLC-UV profiles of monosaccharide compositions in OPS and OPS-S were similar, but they were different from those of OPS-G and OPS-I, suggesting that *in vitro* simulated gastrointestinal digestion also influenced the monosaccharide compositions of OPS. In addition, the monosaccharide compositions of OPS and OPS-S were detected as Rha, Gal, GalA, Glc, GlcA, Man, and Ara, and the monosaccharide compositions of OPS-G and OPS-I were determined as Rha, Gal, GalA, Glc, GlcA, and Man. Ara was a pentose, which was unstable and located in the branching chain of OPS, resulting in an easy degradation by the gastrointestinal digestion (Liu, Wang et al., 2018; Liu, Zhao et al., 2018). The molar ratios of Rha, Gal, GalA, Glc, GlcA, Man, and Ara in OPSs are summarized in Table 2, which varied with the different digestion stages. Results showed that the gastrointestinal digestion significantly affected the types and molar ratios of monosaccharide compositions of OPS.

3.1.3. Changes of FT-IR spectra and degrees of esterification of OPS during digestion

The structure features of OPS, OPS-S, OPS-G, and OPS-I were also analyzed by the FT-IR spectra. As shown in Fig. 3, the FT-IR spectra of OPS, OPS-S, OPS-G, and OPS-I were similar, indicating that different digestion stages had no significant effects on the structure feature of OPS. Briefly, the strong and broad bands at 3419 cm^{-1} were the characteristic stretching absorption peak of the hydroxyl group (Yuan, Lin et al., 2019; Yuan, Li et al., 2019). Bands ranging from 3000 to 2800 cm^{-1} were the C-H stretching vibrations (Fu et al., 2019). The absorption peaks at 1732 cm^{-1} and 1617 cm^{-1} were the C = O stretching vibration of esterified carboxylic groups (-COOR) and carboxylate ion (-COO-) moieties, respectively (Yuan, Lin et al., 2019; Yuan, Li et al., 2019). The absorption peak at 1419 cm^{-1} was due to the stretching vibration of C-H or O-H. Furthermore, two absorption bands at 1617 and 1419 cm^{-1} indicated that the OPSs were all acidic polysaccharides (Yan, Wu, Qiao, Cai, & Ma, 2019). There were no signals at the typical protein bands of 1651 and 1555 cm^{-1}, indicating that few proteins existed in OPSs (Table 1). Furthermore, the FT-IR spectra were also used to determine the degrees of esterification (DE) of OPS, OPS-S, OPS-G, and OPS-I. As shown in Table 1, the DE values of OPS, OPS-S, OPS-G, and OPS-I ranged from 22.09% to 37.99%. The highest DE value (37.99%) was determined in the OPS-G, which might be related to the destruction of free uronic acids by the low pH. However, after gastrointestinal digestion, the DE value in OPS-I (22.09%) decreased significantly when compared with OPS-G ($p < 0.05$), which might be attributed to the destruction of esterified groups by trypsin and alkaline solution (Carnachan et al., 2012). Previous studies have reported that the higher antioxidant activity of natural polysaccharides may be related to a lower DE value (Fu et al., 2019).

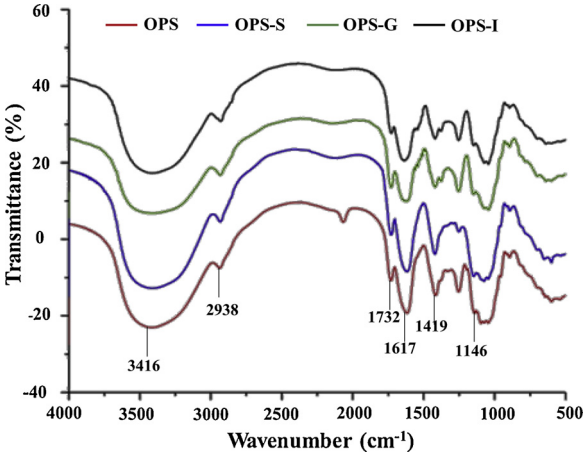

Fig. 3. Changes of FT-IR spectra of okra polysaccharides during digestion. OPS, okra polysaccharides; OPS-S, OPS-G, and OPS-I, OPS digested by saliva digestion, saliva-gastric digestion, and saliva-gastrointestinal digestion, respectively.

3.1.4. Changes of rheological properties of OPS during digestion

Apparent viscosity may affect the binding properties and antioxidant activity of natural polysaccharides (Yuan, Lin et al., 2019; Yuan, Li et al., 2019). Results showed that the apparent viscosities of OPS, OPS-S, OPS-G, and OPS-I solution were influenced by the shear rate (Fig. 4A), respectively. OPS, OPS-S, OPS-G, and OPS-I exhibited both shear-thinning and Newtonian fluid behaviors, respectively. Typical shear-thinning behavior was observed at low shear rates, and the apparent viscosities of OPSs decreased with the increase of shear rates. Then, the apparent viscosities of OPSs remained almost constant at high shear rates, showing the Newtonian plateau. This result was in accordance with a previous study (Nie et al., 2019). Furthermore, the highest apparent viscosity was observed in OPS-G, which might be associated with its highest degree of esterification (Wang et al., 2016).

As shown in Fig. 4B, the storage modulus (G') of each sample was lower than the loss modulus (G″) at low frequencies, indicating the liquid-like behavior of OPS, OPS-S, OPS-G, and OPS-I, respectively. However, the opposite result was observed at high frequencies, suggesting a clear tendency for weak gel properties in OPS, OPS-S, OPS-G, and OPS-I, respectively. The crossover points in OPS, OPS-S, OPS-G, and OPS-I occurring at angular frequencies were detected at 3.16, 3.98, 31.62, and 5.01 rad/s, respectively. After SGD, the crossover points increased following the increase of apparent viscosities of OPS, which might be related to the high degree of esterification. These results suggested that *in vitro* simulated saliva-gastrointestinal digestion could influence the G″ and G′ of OPS.

3.2. Effects of in vitro simulated saliva-gastrointestinal digestion on the antioxidant activities of OPS

The strong antioxidant activity of polysaccharides from okra has been demonstrated in previous studies (Yuan et al., 2020; Zhang, Xiang, Zheng, Yan, & Min, 2018). Therefore, in this study, the effects of *in vitro* simulated saliva-gastrointestinal digestion on the antioxidant activity of

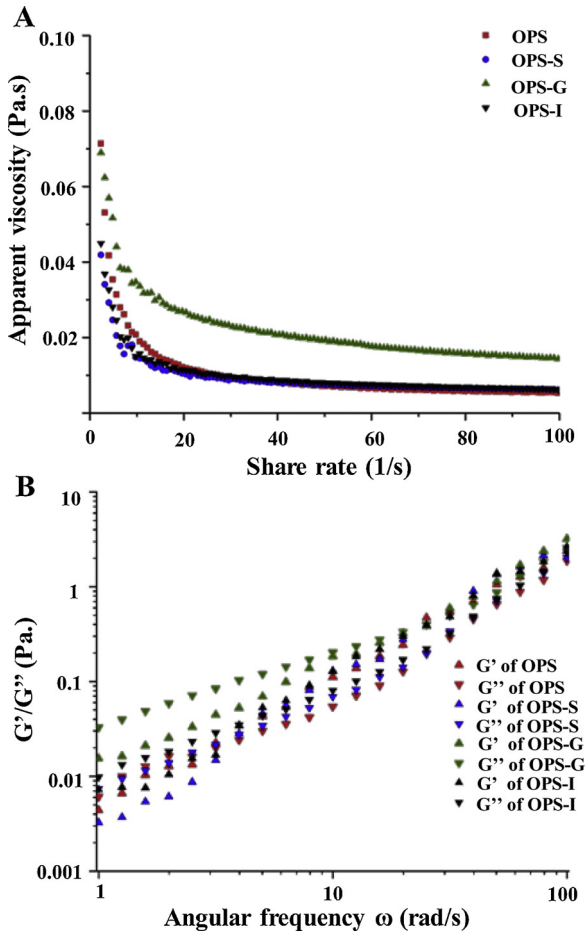

Fig. 4. Changes of rheological properties of okra polysaccharides during digestion.
A, dependences of apparent viscosity on the shear rate; B, plots of storage modulus G′ and loss modulus G″ against frequency; OPS, okra polysaccharides; OPS-S, OPS-G, and OPS-I, OPS digested by saliva digestion, saliva-gastric digestion, and saliva-gastrointestinal digestion, respectively.

OPS were determined. Fig. 5 shows the changes of ABTS and NO radical scavenging activities, as well as ferric reducing antioxidant powers (FRAP) of OPS during digestion. Results showed that OPS exhibited remarkable antioxidant activities when compared with the positive controls, and the saliva-gastrointestinal digestion slightly influenced the antioxidant activities of OPS. The ABTS and NO radical scavenging activities, and FRAP of OPS, OPS-S, OPS-G, and OPS-I showed a dose-dependent manner, respectively. Indeed, the IC_{50} values of ABTS and NO radical scavenging activities of OPS, OPS-S, OPS-G, and OPS-I ranged from 1.47 to 2.16 mg/mL, and from 1.23 to 2.49 mg/mL, respectively. OPSs also exerted strong FRAP values when compared with the positive control, and the absorbances at 593 nm of OPS, OPS-S, OPS-G, and OPS-I ranged from 0.14 to 0.23 at the concentration of 5.0 mg/mL. The ABTS and NO radical scavenging activities of OPS-G were slightly lower than those of other tested samples, which might be related to its higher degree of esterification, resulting in the reduction of antioxidant activities (Yuan, Lin et al., 2019; Yuan, Li et al., 2019).

However, after SGID, the antioxidant activities of OPS-I slightly increased, which might be related to the relatively high contents of uronic acids and conjugated phenolics in OPS-I. The antioxidant activities of OPS, OPS-S, OPS-G, and OPS-I might be related to their chemical characters, unmethylated galacturonic acids (Yuan, Lin et al., 2019; Yuan, Li et al., 2019), and conjugated phenolics (Liu, Wang et al., 2018; Liu, Zhao et al., 2018; Zhu, 2018). Overall, OPS still exhibited strong *in vitro* antioxidant activities after saliva-gastrointestinal

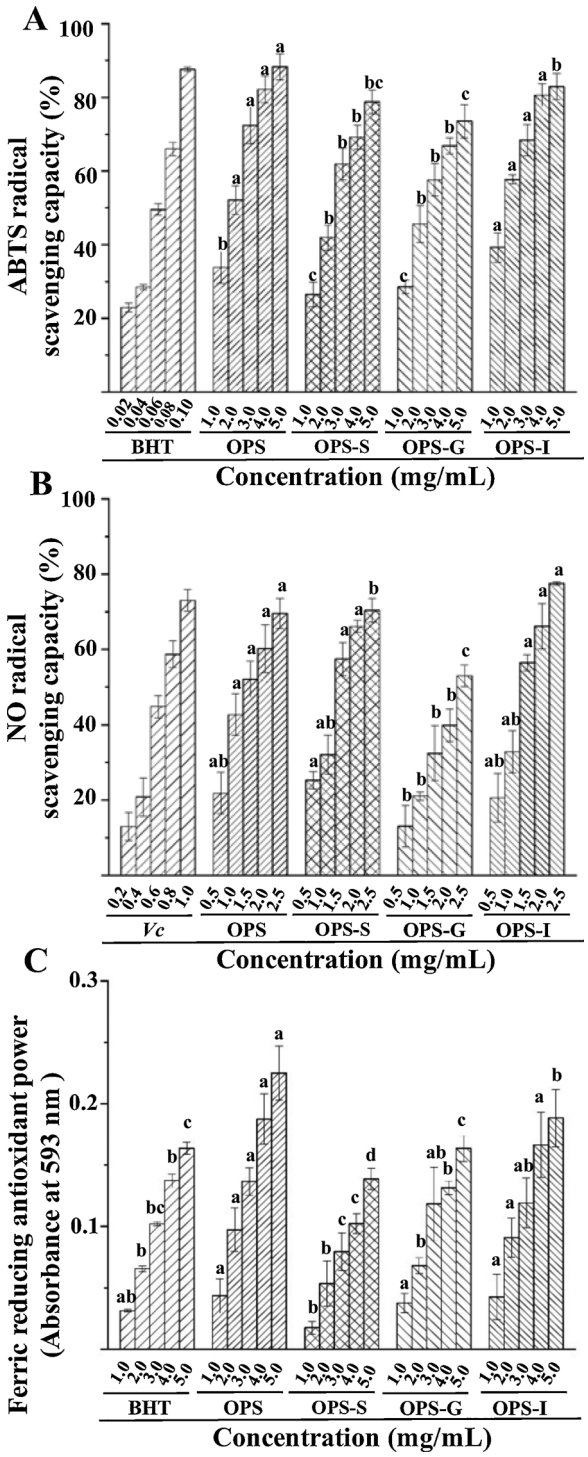

Fig. 5. Changes of ABTS (A) and NO (B) radical scavenging activities, and ferric reducing antioxidant powers (C) of okra polysaccharides during digestion.
OPS, okra polysaccharides; OPS-S, OPS-G, and OPS-I, OPS digested by saliva digestion, saliva-gastric digestion, and saliva-gastrointestinal digestion, respectively; BHT, butylated hydroxytoluene; *Vc*, vitamin C; Means were compared among the samples with the same concentration in each group, and different lowercase letters indicated statistical significance ($p < 0.05$).

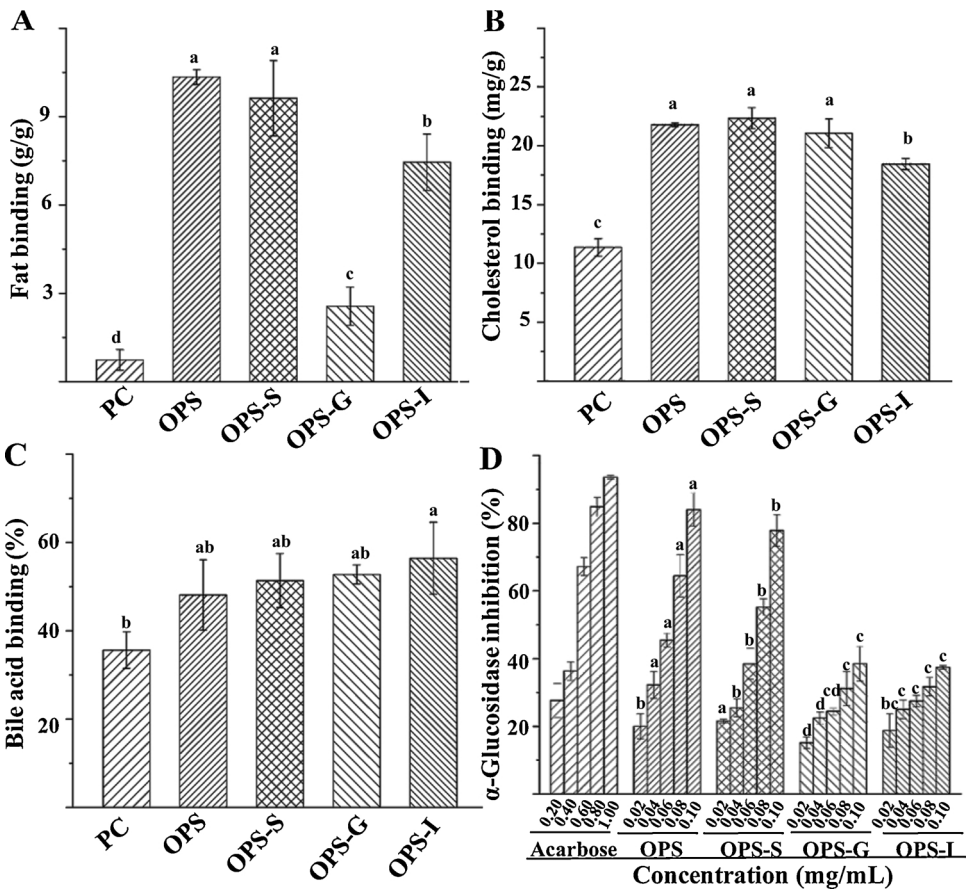

Fig. 6. Changes of fat (A), cholesterol (B), and bile acid (C) binding capacities, as well as inhibitory effects on α-glucosidase (D) of okra polysaccharides during digestion.
OPS, okra polysaccharides; OPS-S, OPS-G, and OPS-I, OPS digested by saliva digestion, saliva-gastric digestion, and saliva-gastrointestinal digestion, respectively.
Carboxymethyl cellulose was used as a positive control in fat binding and cholesterol binding capacities assay, respectively, and cholestyramine was used as a positive control in bile acid binding capacity assay; The error bars are standard deviations. Means were compared among different samples (A–C) or samples with the same concentration in each group (D), and different lowercase letters indicated statistical significance ($p < 0.05$).

digestion.

3.3. Effects of in vitro simulated saliva-gastrointestinal digestion on the binding capacities of OPS

Excessive intake of fat, cholesterol, and bile acids can cause obesity, which can further induce cancer, diabetes, and cardiovascular diseases (Fu et al., 2019). It was reported that the lipid and total serum cholesterol levels of C57BL/6 mice fed with a high-fat diet were reduced after the treatment of okra fruit and okra polysaccharides (Chen et al., 2018). Therefore, it was further investigated about the effects of *in vitro* saliva-gastrointestinal digestion on the binding capacities (fat, cholesterol, and bile-acid binding) of OPS. Fig. 6A–C shows the binding capacities of fat, cholesterol, and bile acid of OPS, OPS-S, OPS-G, and OPS-I, respectively. OPS, OPS-S, OPS-G, and OPS-I exhibited strong *in vitro* binding capacities, and the binding capacities of OPS, OPS-S, OPS-G, and OPS-I with fat, cholesterol, and bile acid ranged from 2.56 to 10.34 g/g, from 18.44 to 22.34 mg/g, and from 48.08 to 52.76%, respectively. Especially, *in vitro* simulated saliva-gastrointestinal significantly influenced their fat binding capacities, and the fat binding capacity of OPS-G was evidently lower than that of others, which might be related to its lower molecular weights (Lin et al., 2018) and narrower molecular weight distributions (Yuan et al., 2020). The bile acid binding capacities of OPS, OPS-S, OPS-G, and OPS-I were similar. Furthermore, although the fat and cholesterol binding capacities of OPS-I were slightly decreased, OPS-I still exerted higher binding capacities in comparison to the positive controls. The initial *in vitro* evidence suggested that OPS had the potential in possibly reducing fat absorption through its binding capacity.

3.4. Effects of in vitro simulated saliva-gastrointestinal digestion on the inhibitory activity on α-glucosidase of OPS

Retarding the absorption of glucose by the suppression of α-glucosidase is used to treat type 2 diabetes (Yuan, Lin et al., 2019; Yuan, Li et al., 2019). Especially, it has been suggested that pectic-polysaccharides from okra fruit possess anti-hyperglycemic activity (Yuan et al., 2020). Therefore, the influences of *in vitro* simulated saliva-gastrointestinal digestion on the α-glucosidase inhibitory effect of OPS were studied. Results showed that OPS possessed strong inhibitory effect on α-glucosidase, and *in vitro* simulated saliva-gastrointestinal digestion also significantly influenced the α-glucosidase inhibitory effect of OPS. As shown in Fig. 6D, OPS, OPS-S, OPS-G, and OPS-I exhibited obviously dose-dependent inhibitory activities on α-glucosidase. The IC_{50} values of α-glucosidase inhibition of OPS, OPS-S, OPS-G, and OPS-I were calculated as 55.63, 64.39, 218.14, and 290.75 μg/mL, respectively. After gastrointestinal digestion, the α-glucosidase inhibitory effects of both OPS-G and OPS-I significantly reduced, which might be attributed to the change of molecular weight distributions and the decrease of total flavonoids (Nie et al., 2019; Shen et al., 2019). It was highlighted that OPS and its digested fractions still exhibited higher inhibitory effects on α-glucosidase when compared with the positive control (acarbose, IC50 = 451.73 μg/mL). The strong α-glucosidase inhibitory effects of OPS, OPS-S, OPS-G, and OPS-I might be owing to their high molecular weights, high degree of esterification, and high contents of uronic acids and total phenolics (Yuan et al., 2020). Due to α-glucosidase is located in the small intestine, OPS after digestion in the small intestine could inhibit the absorption of glucose from the small intestine into the blood, indicating a potential control of postprandial hyperglycemia by OPS (Wang et al., 2018).

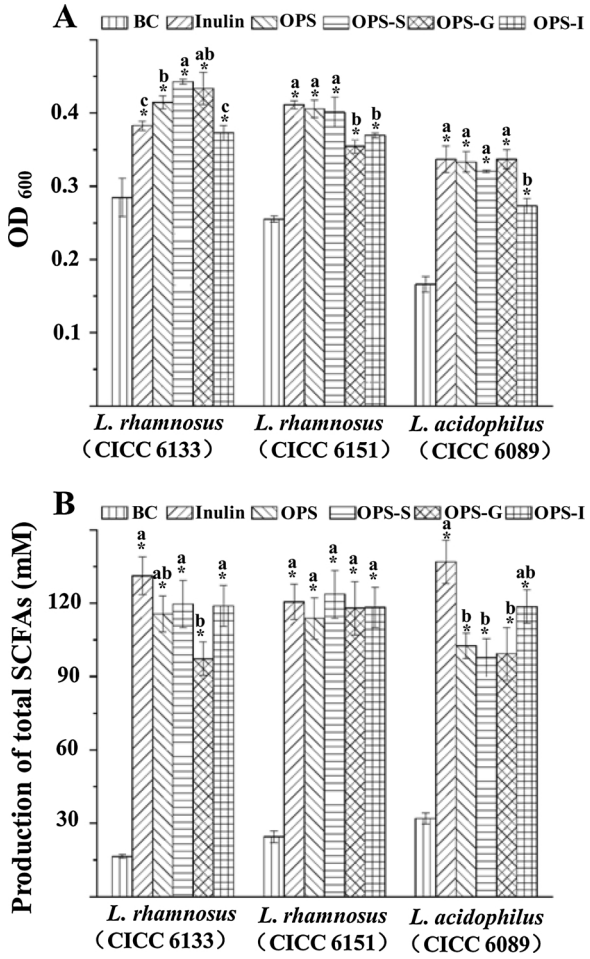

Fig. 7. Effects of OPS and its digestive products on the growth (A) and production of total short-chain fatty acids (B) of three *Lactobacillus* strains.
OPS, okra polysaccharides; OPS-S, OPS-G, and OPS-I, OPS digested by saliva digestion, saliva-gastric digestion, and saliva-gastrointestinal digestion, respectively; The error bars are standard deviations; Significant ($p < 0.05$) differences between blank control and samples are shown by *; Different lowercase letters indicated statistical significance ($p < 0.05$).

3.5. Effects of in vitro simulated saliva-gastrointestinal digestion on the prebiotic activities of OPS

It has been proved that prebiotic activities of natural polysaccharides are essential for their certain health benefits (Huang et al., 2019). The effects of OPS, OPS-S, OPS-G, and OPS-I on the growth of *Lactobacillus* strains were investigated to determine whether OPSs could be metabolized by colon microbiota. The influences of OPSs on the growth of *L. acidophilus* CICC 6089, *L. rhamnosus* CICC 6133, and *L. rhamnosus* CICC 6151 are shown in Fig. 7A. Apparently, all OPSs and inulin could be utilized by *Lactobacillus* strains, and could significantly ($p < 0.05$) promote the growth of three *Lactobacillus* strains. Especially, compared with the positive control (inulin), OPS also exhibited strong prebiotic effects on three *Lactobacillus* strains. Overall, there were no significant changes in the prebiotic activities of OPS after saliva digestion, but the prebiotic activities of OPS-I slightly decreased after gastrointestinal digestion.

The differences determined in prebiotic activities of OPS, OPS-S, OPS-G, and OPS-I might be related to their contents of total polysaccharides, molecular weights, and monosaccharide compositions (Huang et al., 2019). In general, natural polysaccharides with the higher contents of total polysaccharides, the lower molecular weights, and the higher composition of arabinose and galactose may exert better prebiotic activity (Huang et al., 2019). Furthermore, Fig. 7B shows the production of total SCFAs from three *Lactobacillus* strains. Results revealed that all OPSs and inulin could significantly promote the production of total SCFAs from *L. rhamnosus* CICC 6133, *L. rhamnosus* CICC 6151, and *L. acidophilus* CICC 6089. There were no significant changes in total SCFAs produced from three *Lactobacillus* strains cultivated with OPS after simulated gastrointestinal digestion. OPS still exhibited strong effects on promoting the production of total SCFAs from *Lactobacillus* strains after *in vitro* simulated gastrointestinal digestion. Besides, compared with the positive control (inulin), OPS-I also exhibited strong abilities to promote the production of SCFAs from *Lactobacillus* strains, confirming that OPS and its digestive products could be utilized by probiotic bacteria to sustain survival and metabolic activity.

4. Conclusions

In this study, the *in vitro* simulated saliva-gastrointestinal digestion on the physicochemical properties and bioactivities of okra polysaccharides were investigated. Physicochemical properties of okra polysaccharides changed obviously during saliva-gastrointestinal digestion. Although the binding capacities, inhibitory effects on α-glucosidase, and prebiotic effects of okra polysaccharides were decreased after saliva-gastrointestinal digestion, the digestive products still exhibited strong bioactivities when compared with the positive controls. Therefore, this study can contribute to a better understanding of the potential digestion mechanism of okra polysaccharides, which should have important implications for future studies on the development of okra polysaccharides as functional foods and medicines.

CRediT authorship contribution statement

Qin Yuan: Data curation, Formal analysis, Investigation, Resources, Software, Writing - original draft. **Yuan He:** Formal analysis, Investigation, Validation, Resources, Software, Writing - original draft. **Pan-Yin Xiang:** Formal analysis, Investigation. **Sheng-Peng Wang:** Formal analysis, Resources. **Zheng-Wen Cao:** Formal analysis, Investigation. **Tao Gou:** Formal analysis, Investigation. **Miao-Miao Shen:** Formal analysis, Investigation. **Li Zhao:** Formal analysis, Investigation, Software. **Wen Qin:** Resources. **Ren-You Gan:** Formal analysis, Funding acquisition, Methodology, Writing - review & editing. **Ding-Tao Wu:** Conceptualization, Data curation, Formal analysis, Funding acquisition, Methodology, Supervision, Project administration, Writing - review & editing.

Declaration of Competing Interest

The authors declare that there are no conflicts of interest.

Acknowledgements

This work was supported by the National Natural Science Foundation of China (grant number 31901690), the China Central Public-interest Scientific Institution Basal Research Fund (grant number Y2020XK05), the Scientific Research Fund Project of Department of Science and Technology of Sichuan Province (grant number 2018JY0149), and the Scientific Research Foundation of Sichuan Agricultural University (grant number 03120321).

References

Carnachan, S. M., Bootten, T. J., Mishra, S., Monro, J. A., & Sims, I. M. (2012). Effects of simulated digestion *in vitro* on cell wall polysaccharides from kiwifruit (*Actinidia* spp.). *Food Chemistry, 133*(1), 132–139.
Chen, C., Zhang, B., Fu, X., You, L. J., Abbasi, A. M., & Liu, R. H. (2016). The digestibility of mulberry fruit polysaccharides and its impact on lipolysis under simulated saliva, gastric and intestinal conditions. *Food Hydrocolloids, 58*, 171–178.
Chen, G. J., Xie, M. H., Wan, P., Chen, D., Ye, H., Chen, L. G., et al. (2018). Digestion

under saliva, simulated gastric and small intestinal conditions and fermentation *in vitro* by human intestinal microbiota of polysaccharides from Fuzhuan brick tea. *Food Chemistry, 244*, 331–339.
Chen, J., Liang, R. H., Liu, W., Liu, C. M., Li, T., Tu, Z. C., et al. (2012). Degradation of high-methoxyl pectin by dynamic high pressure microfluidization and its mechanism. *Food Hydrocolloids, 28*(1), 121–129.
Di, T., Chen, G. J., Sun, Y., Ou, S., Zeng, X. X., & Ye, H. (2018). *In vitro* digestion by saliva, simulated gastric and small intestinal juices and fermentation by human fecal microbiota of sulfated polysaccharides from *Gracilaria rubra*. *Journal of Functional Foods, 40*, 18–27.
Fu, Y., Yuan, Q., Lin, S., Liu, W., Du, G., Zhao, L., et al. (2019). Physicochemical characteristics and biological activities of polysaccharides from the leaves of different loquat (*Eriobotrya japonica*) cultivars. *International Journal of Biological Macromolecules, 135*, 274–281.
Gao, H., Zhang, W. C., Wu, Z. Y., Wang, H. Y., Hui, A. L., Meng, L., et al. (2018). Preparation, characterization and improvement in intestinal function of polysaccharide fractions from okra. *Journal of Functional Foods, 50*, 147–157.
Guo, H., Yuan, Q., Fu, Y., Liu, W., Su, Y. H., Liu, H., et al. (2019). Extraction optimization and effects of extraction methods on the chemical structures and antioxidant activities of polysaccharides from snow chrysanthemum (*Coreopsis tinctoria*). *Polymers, 11*, 215.
Hosseini, S. S., Khodaiyan, F., Kazemi, M., & Najari, Z. (2019). Optimization and characterization of pectin extracted from sour orange peel by ultrasound assisted method. *International Journal of Biological Macromolecules, 125*, 621–629.
Hu, J. L., Nie, S. P., Min, F. F., & Xie, M. Y. (2013). Artificial simulated saliva, gastric and intestinal digestion of polysaccharide from the seeds of *Plantago asiatica* L. *Carbohydrate Polymers, 92*(2), 1143–1150.
Hu, X. T., & Goff, H. D. (2018). Fractionation of polysaccharides by gradient non-solvent precipitation: A review. *Trends in Food Science & Technology, 81*, 108–115.
Huang, F., Liu, H. J., Zhang, R. F., Dong, L. H., Liu, L., Ma, Y. X., et al. (2019). Physicochemical properties and prebiotic activities of polysaccharides from longan pulp based on different extraction techniques. *Carbohydrate Polymers, 206*, 344–351.
Hur, S. J., Lim, B. O., Decker, E. A., & McClements, D. J. (2011). *In vitro* human digestion models for food applications. *Food Chemistry, 125*(1), 1–12.
Li, W. W., Wang, C., Yuan, G. Q., Pan, Y. X., & Chen, H. X. (2018). Physicochemical characterisation and α-amylase inhibitory activity of tea polysaccharides under simulated salivary, gastric and intestinal conditions. *International Journal of Food Science & Technology, 53*(2), 423–429.
Lin, S., Guo, H., Lu, M., Lu, M. Y., Gong, J., Wang, L., et al. (2018). Correlations of molecular weights of β-glucans from Qingke (Tibetan hulless barley) to their multiple bioactivities. *Molecules, 23*, 1710.
Liu, J., Wang, X. C., Yong, H. M., Kan, J., & Jin, C. H. (2018). Recent advances in flavonoid-grafted polysaccharides: Synthesis, structural characterization, bioactivities and potential applications. *International Journal of Biological Macromolecules, 116*, 1011–1025.
Liu, J., Zhao, Y. P., Wu, Q. X., John, A., Jiang, Y. M., Yang, J. L., et al. (2018). Structure characterisation of polysaccharides in vegetable "okra" and evaluation of hypoglycemic activity. *Food Chemistry, 242*, 211–216.
Nie, X. R., Li, H. Y., Du, G., Lin, S., Hu, R., Li, H. Y., et al. (2019). Structural characteristics, rheological properties, and biological activities of polysaccharides from different cultivars of okra (*Abelmoschus esculentus*) collected in China. *International Journal of Biological Macromolecules, 139*, 459–467.
Olawuyi, I. F., Kim, S. R., Hahn, D., & Lee, W. Y. (2020). Influences of combined enzyme-ultrasonic extraction on the physicochemical characteristics and properties of okra polysaccharides. *Food Hydrocolloids, 100*, 105396.
Quan, W., Tao, Y. D., Lu, M., Yuan, B., Chen, J., Zeng, M. M., et al. (2018). Stability of the phenolic compounds and antioxidant capacity of five fruit (apple, orange, grape, pomelo and kiwi) juices during *in vitro*-simulated gastrointestinal digestion. *International Journal of Food Science & Technology, 53*(5), 1131–1139.
Shen, D. D., Li, X., Qin, Y. L., Li, M. T., Han, Q. H., Zhou, J., et al. (2019). Physicochemical properties, phenolic profiles, antioxidant capacities, and inhibitory effects on digestive enzymes of okra (*Abelmoschus esculentus*) fruit at different maturation stages. *Journal of Food Science and Technology, 56*(3), 1275–1286.
Wang, C., Li, W. W., Chen, Z. Q., Gao, X. D., Yuan, G. Q., Pan, Y. X., et al. (2018). Effects of simulated gastrointestinal digestion *in vitro* on the chemical properties, antioxidant activity, alpha-amylase and alpha-glucosidase inhibitory activity of polysaccharides from *Inonotus obliquus*. *Food Research International, 103*, 280–288.
Wang, W. J., Ma, X. B., Jiang, P., Hu, L. L., Zhi, Z. J., Chen, J. L., et al. (2016). Characterization of pectin from grapefruit peel: A comparison of ultrasound-assisted and conventional heating extractions. *Food Hydrocolloids, 61*, 730–739.
Wu, D. T., Guo, H., Lin, S., Lam, S. C., Zhao, L., Lin, D. R., et al. (2018). Review of the structural characterization, quality evaluation, and industrial application of *Lycium barbarum* polysaccharides. *Trends in Food Science & Technology, 79*, 171–183.
Wu, D. T., Lam, S. C., Cheong, K. L., Wei, F., Lin, P. C., Long, Z. R., et al. (2016). Simultaneous determination of molecular weights and contents of water-soluble polysaccharides and their fractions from *Lycium barbarum* collected in China. *Journal of Pharmaceutical and Biomedical Analysis, 129*, 210–218.
Wu, D. T., Meng, L. Z., Wang, L. Y., Lv, G. P., Cheong, K. L., Hu, D. J., et al. (2014). Chain conformation and immunomodulatory activity of a hyperbranched polysaccharide from *Cordyceps sinensis*. *Carbohydrate Polymers, 110*(38), 405–414.
Yan, J. K., Wu, L. X., Qiao, Z. R., Cai, W. D., & Ma, H. (2019). Effect of different drying methods on the product quality and bioactive polysaccharides of bitter gourd (*Momordica charantia* L.) slices. *Food Chemistry, 271*, 588–596.
Yuan, Q., Lin, S., Fu, Y., Nie, X. R., Liu, W., Su, Y., et al. (2019). Effects of extraction methods on the physicochemical characteristics and biological activities of polysaccharides from okra (*Abelmoschus esculentus*). *International Journal of Biological Macromolecules, 127*, 178–186.
Yuan, Y. Q., Li, C., Zheng, Q. W., Wu, J. X., Zhu, K. X., Shen, X. R., et al. (2019). Effect of simulated gastrointestinal digestion *in vitro* on the antioxidant activity, molecular weight and microstructure of polysaccharides from a tropical sea cucumber (*Holothuria leucospilota*). *Food Hydrocolloids, 89*, 735–741.
Yuan, Q., He, Y., Xiang, P. Y., Huang, Y. J., Cao, Z. W., Shen, S. W., et al. (2020). Influences of different drying methods on the structural characteristics and multiple bioactivities of polysaccharides from okra (*Abelmoschus esculentus*). *International Journal of Biological Macromolecules, 147*, 1053–1063.
Zhang, T., Xiang, J. L., Zheng, G. B., Yan, R. Q., & Min, X. (2018). Preliminary characterization and anti-hyperglycemic activity of a pectic polysaccharide from okra (*Abelmoschus esculentus* (L.) Moench). *Journal of Functional Foods, 41*, 19–24.
Zhu, F. (2018). Interactions between cell wall polysaccharides and polyphenols. *Critical Reviews in Food Science and Nutrition, 58*(11), 1808–1831.
Zhu, K. X., Yao, S. W., Zhang, Y. J., Liu, Q. B., Xu, F., Wu, G., et al. (2019). Effects of *in vitro* saliva, gastric and intestinal digestion on the chemical properties, antioxidant activity of polysaccharide from *Artocarpus heterophyllus Lam.* (Jackfruit) Pulp. *Food Hydrocolloids, 87*, 952–959.